Contr. Mineral. and Petrol. 43, 163—194 (1974)

$^{238}U/^{206}Pb$-$^{235}U/^{207}Pb$-$^{232}Th/^{208}Pb$ Zircon Geochronology in Alpine and Non-Alpine Environment

Claude J. Allègre, and Francis Albarède

Groupe de Recherches Géochimiques Louis Barrabé, Institut de Physique du Globe et Département des Sciences de la Terre, Université de Paris 6 et 7 (France)

Marc Grünenfelder and Viktor Köppel

Laboratory for Isotope Geology and Masspectrometry, Swiss Federal Institute of Technology, Zürich, Switzerland

Received July 23, 1973

Abstract. Based on regular arrays in a U-Pb diagram of data points of zircons from polymetamorphic rocks of the Alps quantitative models are developed that include several episodic lead losses, continuous lead losses during discrete periods and combinations of both.

The data from the Alps can be explained by assuming an initial age of the zircons of 2000 and/or 2500–2600 m.y. and three episodic lead losses 520–580 m.y., 300 m.y. and 30 m.y. ago with regionally varying intensities of the events as can be seen from the efficiency parameters which define the shape of the discordia. On the other hand, zircon data from North American basement rocks satisfy a model assuming a discrete interval of continuous lead loss that starts with the time of uplift of the rocks.

The Th-U-Pb diagrams are valuable for recognising whether the history of the zircons and their host rock is a complex one or not which is not always noticeable in a U-Pb diagram.

1. Introduction

Zircon ^{238}U-^{206}Pb and ^{235}U-^{207}Pb ages are generally discordant. For such cases Ahrens (1955) has shown that the ratios $^{206}Pb/^{238}U$ and $^{207}Pb/^{235}U$ are frequently linearily related.

Using the $^{206}Pb/^{238}U$-$^{207}Pb/^{235}U$ diagram, Wetherill (1956) constructed the so called concordia curve, the locus of concordant ages. It is defined by the parametric equations:

$$r_{\lambda_8} = {}^{206}Pb/^{238}U = (e^{\lambda_8 T} - 1)$$

$$r_{\lambda_5} = {}^{207}Pb/^{235}U = (e^{\lambda_5 T} - 1)$$

where λ_8 and λ_5 are the decay constants for ^{238}U and ^{235}U respectively. The empirical straight line observed by Ahrens intersects the concordia curve at two points (Fig. 1a). We denote by T^* the upper and by T_1^* the lower intercept. According to Wetherill (1956), T^* corresponds for fractions of a cogenetic zircon population to the primary age T of the population and T_1^* is the time T_1 of an episodic event during which the U-Pb systems are open for a short duration compared to T or T^* (Fig. 1b).

By analysing zircons separated from one block of rock and by assuming that these zircons are cogenetic, Silver and his coworkers have obtained strong evidence for Wetherill's model (Silver and Deutsch, 1963).

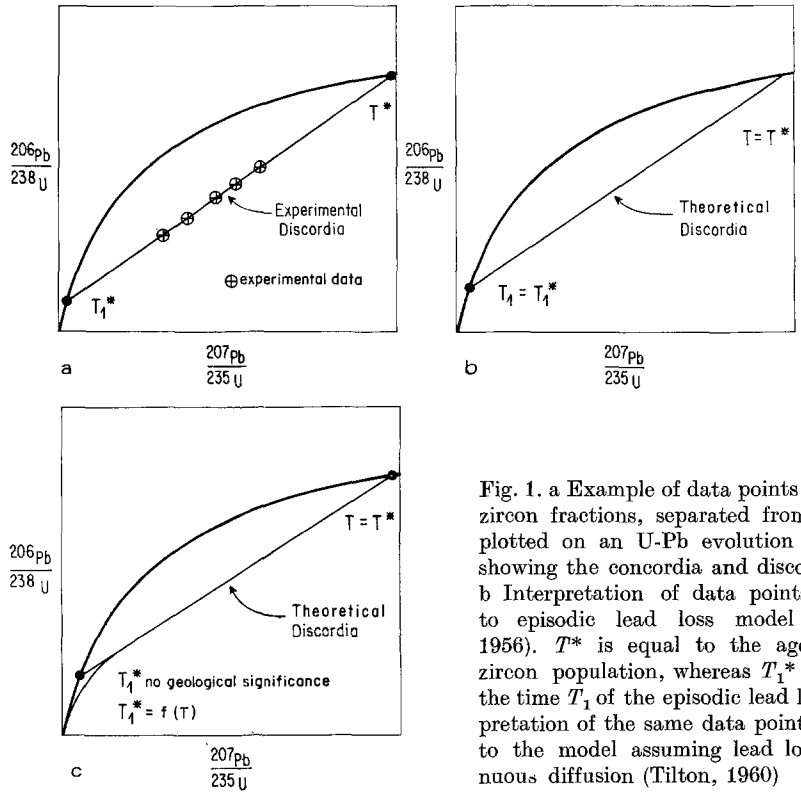

Fig. 1. a Example of data points for different zircon fractions, separated from one suite, plotted on an U-Pb evolution diagram, showing the concordia and discordia curves. b Interpretation of data points according to episodic lead loss model (Wetherill, 1956). T^* is equal to the age T of the zircon population, whereas T_1^* is equal to the time T_1 of the episodic lead loss. c Interpretation of the same data points according to the model assuming lead loss by continuous diffusion (Tilton, 1960)

Tilton (1960) pointed out that it is often difficult to associate T_1^* with a known geological event at T_1. To solve this problem, he proposed a model according to which zircons lose some Pb continuously. T_1^* has therefore no geological significance, whereas T^* corresponds to the primary age T (Fig. 1c).

Wasserburg (1963) proposed a similar continuous diffusion model with a diffusion coefficient increasing with time.

Silver (1963) and Catanzaro (1963) give, however, examples which fit neither Tilton's nor Wasserburg's model. On the basis of the observed arrays of discordant U-Pb data points it was in most cases impossible to decide, whether continuous or episodic Pb loss was operative.

An interpretation based only on a continuous diffusion or a monoepisodic disturbance model must appear unsatisfactory. Are inherent heterogeneities of the zircons and /or a complex geological history not reflected in the zircon age patterns? Steiger and Wasserburg (1969) have assumed that a complex disturbance, e. g. two episodic events, will lead to a scatter of the observed data points in a $r_{\lambda_8} - r_{\lambda_5}$ diagram. An effort to understand complex cases was made by Wetherill (1963), but apparently with limited resonance.

In a generalisation of the concordia concept Allègre (1965, 1967) combined the ^{235}U-^{207}Pb with the ^{232}Th-^{208}Pb system. The experimental discordias have variable slopes, however, they never intersect the concordia at two points. The diagram was

used to support the episodic disturbance rather than the continuous diffusion model. Steiger and Wasserburg (1966) used the diagram to interprete the Sandia granite zircon data points and proposed a new model according to which zircons are mixtures of two phases with different U/Th ratios. For this example they assume an episodic lead loss, however they admit the possibility of a continuous loss with different diffusion constants for the two phases.

In spite of all these efforts we are still left without answers concerning the value of episodic or continuous lead loss models. In fact, the question of episodic or continuous loss of lead, uranium or thorium, bears not only on the problems of the geological validity of T_1* and of a physico-chemical explanation of the mechanism of open systems, but also on the important problem whether the U-Th-Pb age patterns reflect the geological history of a zircon population and its host rock.

The results of zircon analyses from the central part of the Alps lead to a new insight into this problem. The geological history of the Alps is complicated, yet the zircon data points still exhibit some regularities in the $r_{\lambda_8}-r_{\lambda_5}$ diagram. The experimentally determined discordia curves are more complicated than those for zircons of the Precambrian of North-America but they are nevertheless smooth (Figs. 2, 3).

This paper explores quantitatively a complex geological situation in the light of the results from the Alps and compares them with results obtained from the Precambrian of North America.

2. Zircon U-Pb Age Patterns of the Alps

The pre-Mesozoic rocks of the Alps are polymetamorphic. From field geology and geochronology we know of the existence of several tectonometamorphic events: in the central part of the Alps the latest events took place 40 to 15 m. y. ago. The Hercynian orogeny occured about 300 m. y. ago, and in addition we know of one or two pre-Hercynian events between 420–600 m. y. Petrographic observations have shown that in the central Alps the Alpine orogeny caused high grade regional metamorphism only in the central Penninic-Lepontic region (P. Niggli, 1936; E. Wenk, 1943, 1970; E. Niggli, 1970).

Zircon studies by Grauert and Arnold (1968) in the Gotthard and Silvretta regions, by Gruenenfelder and Koeppel in the Penninic region (analytical data compiled in Appendix II., Table 1, sample description in Table 2), by Pidgeon *et al.* (1970) and by Koeppel and Gruenenfelder (1971) in the Southern Alps, have shown unusual patterns in the U-Pb evolution diagram (Figs. 2–5). The important point is that in spite of the complex geological history the data points *do not scatter much in the* $r_{\lambda_8}-r_{\lambda_5}$ *diagram*. In this respect the following general comments can be made:

a) Paragneiss zircon suites yield highly discordant age patterns which, for a given region, are very similar.

b) Zircons from associated orthogneisses have younger, almost concordant ages (e. g. Fig. 2a, 3); in some cases zircons from granitic gneisses show drastic post-Hercynian Pb losses.

c) On a large scale, a relationship is noticeable between the intensity of the Alpine event and the apparent zircon ages: this is illustrated by comparing of the

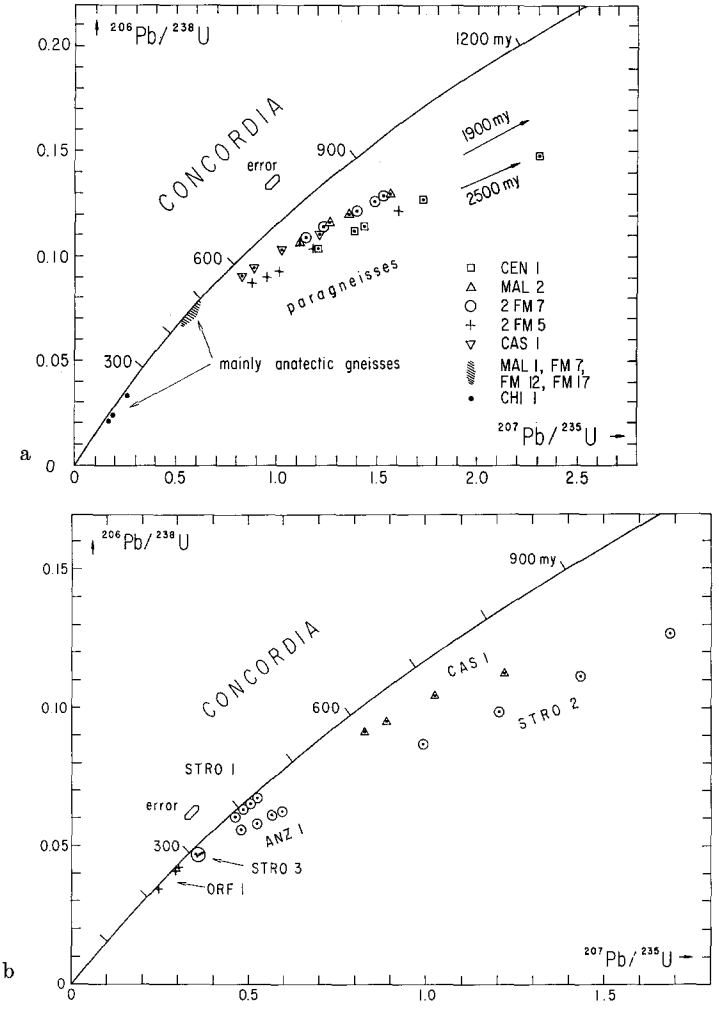

Fig. 2. a Zircon data points from the Southern Alps (Ceneri and Val Colla zones) (Pidgeon *et al.* 1970; Koeppel and Gruenenfelder, 1971) b Zircon data points from paragneisses of upper amphibolite to granulite facies of the Ivrea Zone (STRO 2, STRO 3, and ANZ 1), and a postmetamorphic granite (ORF 1) from the Ceneri zone, Southern Alps. The age patterns show the dominating influence of a Hercynian event (Koeppel, in preparation). The data points of the paragneiss zircon sample CAS 1 and a migmatic orthogneiss (STRO 1) serve as a reference pattern showing a dominating prehercynian event in the neighbouring Ceneri-zone

age patterns of the Silvretta region (Fig. 3) and the Southern Alps (Fig. 2a and b) where the influence of the Alpine event is not intense, with the Penninic region, where the Alpine metamorphism reached its highest grade (Fig. 4).

d) Paradoxically, on a small scale the degree of discordance appears not to be correlated with the intensity of the Alpine metamorphism (Fig. 5).

The results cannot be fully explained by the classical models of continuous or mono-episodic lead loss. For this reason complex models will be presented here, compatible with the geological history of a given region.

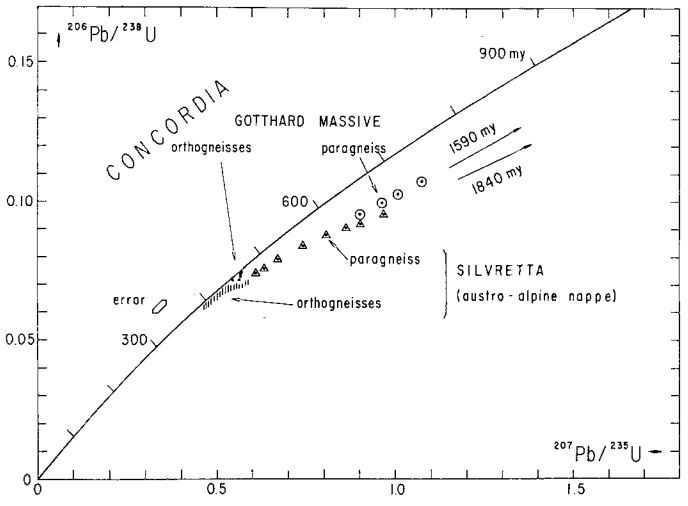

Fig. 3. Zircon data points from the crystalline core of the austro-alpine Silvretta nappe and the Gotthard massive (Grauert and Arnold, 1968)

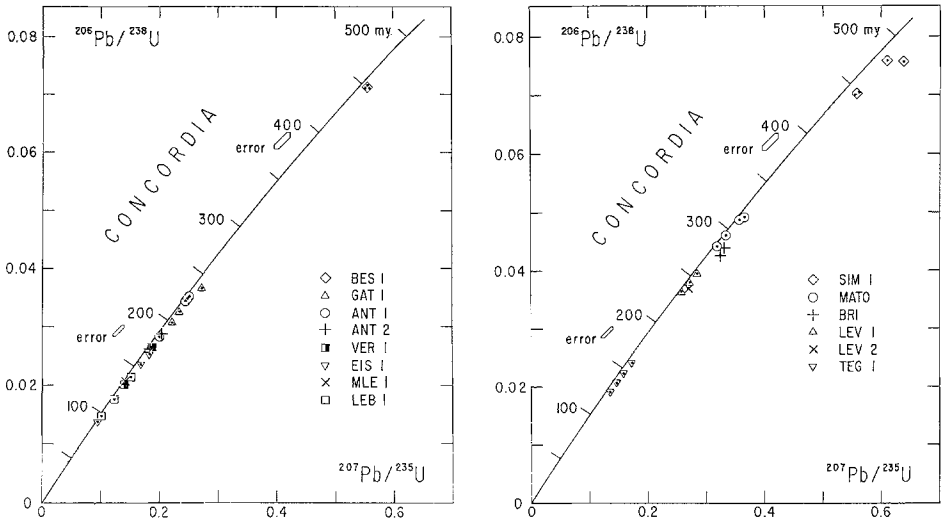

Fig. 4. a Zircon data points from the orthogneiss cores of the nappes from the Simplon area. b Zircon data points from the central Penninic area. For sample description see appendix II

3. Theoretical Model Calculations for the U-Pb Systems

3.1. Preliminary Remarks and Basic Assumptions

It is assumed that Pb or U loss processes can be described by a first order kinetic equation similar to that used by Damon (1968) for the K—Ar-system. Several arguments support this assumption:

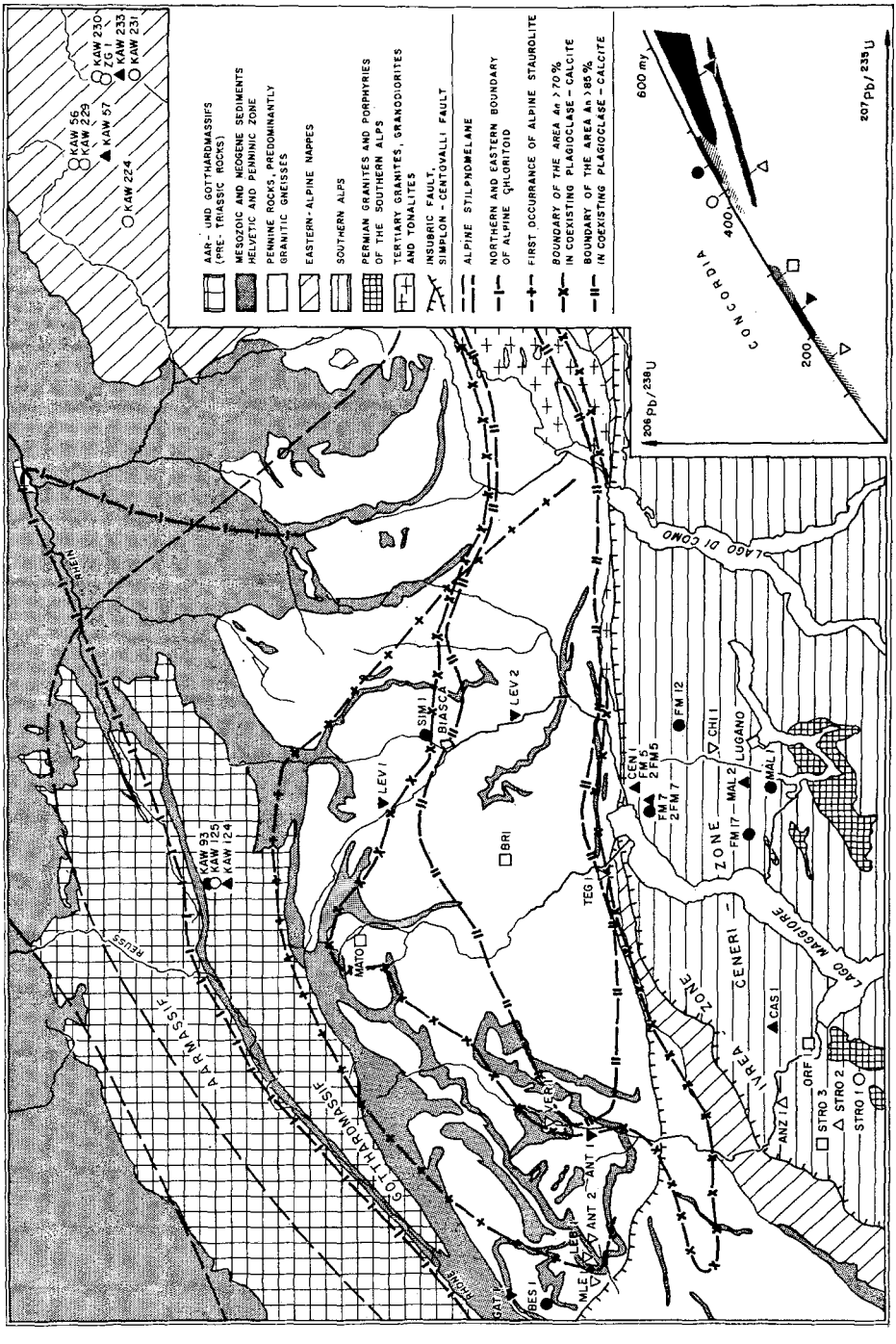

Fig. 5. Tectonic sketch map showing the sample locations

a) It has been shown that the degree of discordance is not a simple function of $1/a^2$ where a is the radius of the diffusion sphere, but rather depends on different parameters, such as trace element concentrations. Hence the rate of loss is not only determined by a volume diffusion process.

b) Using a kinetic model, Craig (1968) has satisfactorily interpreted the results of laboratory experiments made by Pidgeon, O'Neil and Silver (1966).

c) The discordia curves for the Tilton (1960) or the Wasserburg (1963) model can be fairly accurately reproduced by kinetic models (Ulrych, 1963).

The evolution of a system at time t can be described by the two equations:

$$\frac{dP}{dt} = -\lambda P - J_P P$$

$$\frac{dF}{dt} = \lambda P - J_F F$$

where λ is the decay constant of the parent isotope. F and P are the concentrations of daughter and parent atoms, J_P and J_F are the rate constants for daughter and parent loss as a function of time.

Combining these two equations according to Wetherill and putting $r = F/P$, $\xi = J_P - J_F$, we get:

$$\frac{dr}{dt} = \lambda + (\lambda + \xi)\, r.$$

We consider the history of a zircon suite as a sequence of time intervals during which the behaviour of the parent-daughter system remains fixed, the condition being $\xi =$ constant. The parameter ξ therefore conveys the history of a zircon suite. Starting with the ratio $r\ (Tj)$ at time Tj, we integrate the fundamental equation to obtain the ratio $r\ (T_{j+1})$ at time T_{j+1}.

$$r(T_{j+1}) = \frac{\lambda}{\lambda + \xi}\{e^{(\lambda+\xi)(T_j - T_{j+1})} - 1\} + r(T_j)\, e^{(\lambda+\xi)(T_j - T_{j+1})}$$

For an interval 3 different types of behaviour of the parent-daughter system may be envisaged:

a) The system remains closed from T_j to T_{j+1}, then $\xi = 0$.

b) The system loses U and Pb at a constant rate such as $\xi = C^{te}$ with $\xi \propto \lambda$. As usual, $J_P < J_F$, so ξ is negative.

c) The system undergoes such a strong U-Pb loss during the time interval $T_j - T_{j+1} = \Delta_j$, that the radioactive decay may be neglected. Defining $J_{T_j} = \xi$ with $-J_{T_j} \gg \lambda$

$$r(T_{j+1}) = r(T_j) \exp(J_{T_j} \Delta_j).$$

For short Δ_j and large J_{T_j}, this equation compares with the one by Whetherill (1956) by putting

$$R_j = r(T_j - \Delta_j)/r(T_j).$$

Multi-interval models can be derived from the three basic equations (Appendix I), or generated on a computer.

If these complex models involve a continuous loss and an episodic event, the episodic parameter J_{T_j} obeying $Rj = \exp(J_{T_j} \Delta_j)$ is related to the continuous loss parameter ξ by $J_{T_j} = K_{T_j} \xi$ where K_{T_j} is the intensity factor of the *j-th* episodic loss.

For models with more than one episodic loss, we follow the same procedure:

$$R_j = \exp(K_{T_j} \Delta_j \xi), \qquad R_n = \exp(K_{T_n} \Delta_n \xi).$$

Defining $\varphi_j = K_{T_j} \Delta_j / K_{T_n} \Delta_n$, we get $R_j = R_n^{\varphi_j}$ which holds even if $\xi \to 0$.

For a suite of cogenetic zircons, we will consider three cases:

a) n-episodic models where closed system intervals are separated by n episodic losses. All φ_j are assumed to be constant and the present day r becomes a function of a single variable R_n.

b) multistage continuous loss models with alternating intervals of closed and continuous loss regime.

c) multistage continuous + n-episodic loss models which are a combination of models *a* and *b*. In this case R_n is related to the continuous loss parameter by $R_n = \exp(K_{T_n} \Delta_n \xi)$, or by putting $A = K_{T_n} \Delta_n \lambda_8$

$$R_n = \exp(-A \cdot n)$$

with n integer positive.

The integrated equation for a complex history has the general parametric form:

$$r = \Phi\{\lambda, K_{T_n} \Delta_n, \xi, \varphi_1, \varphi_2, \ldots, \varphi_{n-1}\}$$

in which $\varphi_1, \varphi_2, \ldots, \varphi_{n-1}$ are constants and the only parameter is ξ. So it is possible to draw, in the r_{λ_8} vs. r_{λ_5} diagram, the discordia curve fixing the constants and giving several values for parameter A.

Three limiting cases have been calculated:

3.2. Triepisodic Model Disturbance,

In which three episodic tectonometamorphic loss events occur in the history of zircon populations (Fig. 6) ($\varphi' = K_{T_1} \Delta_1 / K_{T_3} \Delta_3$, $\varphi = K_{T_2} \Delta_2 / K_{T_3} \Delta_3$). Fig. 7 shows these calculations.

Fig. 8 shows that it is possible to explain the experimental results of the Alps with a triepisodic model.

3.3. Multistage Continuous Loss Model (MC).

In the continuous diffusion models proposed by Tilton (1960) and Wasserburg (1963) it is assumed that the lead loss occurs between the time of zircon formation and today. Thus, the behaviour of the parent-daughter system of a zircon population is assumed to be independant of the p-T history of the zircon suite. In contrast we may assume that continuous loss occurs only during definite intervals of the zircon history:

a) after their formation the rocks are held at evelated temperature and fluid pressure and consequently the U-Pb system in zircons is partially open. During a short tectonic episode (uplift and/or compression) at T_1 the rocks rapidly rise to the surface. At low temperature conditions, zircons may almost behave as closed systems (Fig. 9a).

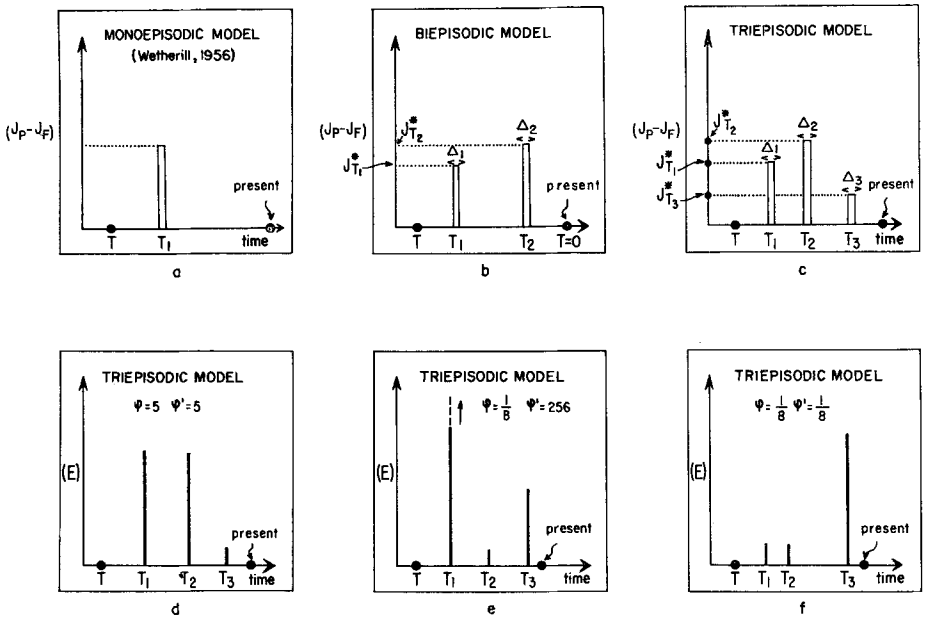

Fig. 6. a–f. Mono-, bi-, and triepisodic loss models showing $(J_P - J_F)$ versus time. The relative efficiencies E of the event plotted versus time for the triepisodic loss models, in which φ and φ' are variable

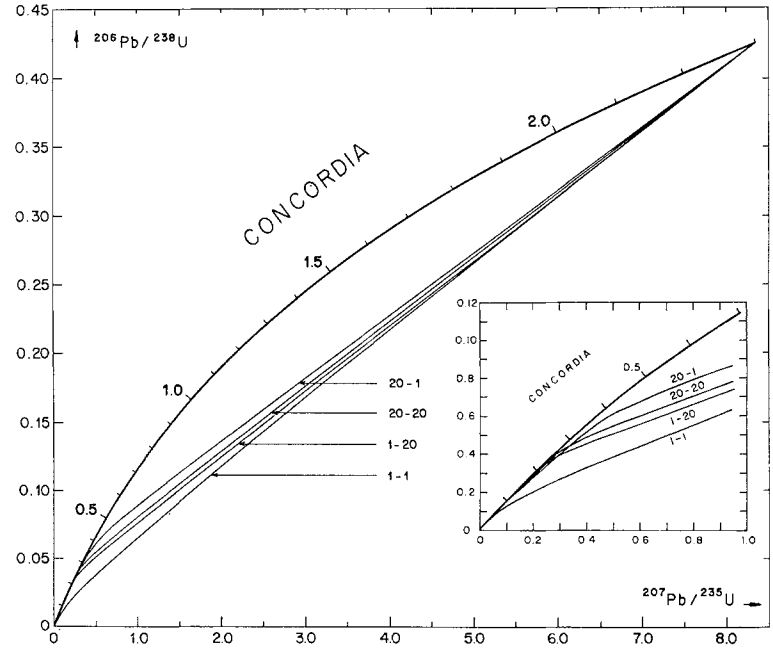

Fig. 7. Calculated discordias for a triepisodic loss model. $T = 2300$ m. y., $T_1 = 500$ m. y., $T_2 = 300$ m. y., $T_3 = 30$ m. y. The values of φ and φ' are defined by

$$\varphi' = \frac{K_{T_1} \Delta_1}{K_{T_3} \Delta_3}, \qquad \varphi = \frac{K_{T_2} \Delta_2}{K_{T_3} \Delta_3}.$$

The indices of each curve correspond to the values chosen for φ' and φ respectively

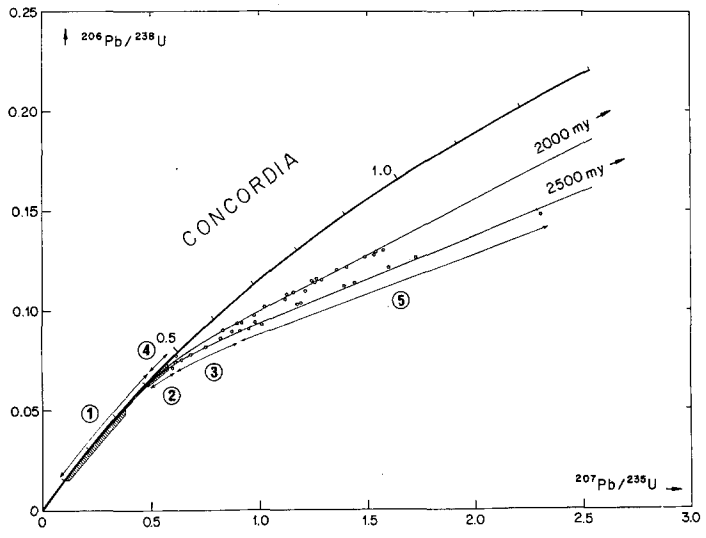

Fig. 8. Best fit between triepisodic loss model and results from the central part of the Swiss Alps. The discordias are calculated for $T = 2000$ m. y., and 2500 m. y., $T_1 = 560$ m. y., $T_2 = 300$ m. y., $T_3 = 30$ m. y. $\varphi' = 200$, $\varphi = 20$. *1* Penninic region (see Table 1. + 2.). *2* Gotthard and Silvretta orthogneisses. *3* Silvretta paragneisses (2. + 3.: Grauert a. Arnold, 1968). *4* Southern Alps orthogneisses (4. + 5.: Pidgeon *et al.*, 1970). *5* Southern Alps, (Köppel a. Grünenfelder, 1971) and Gotthard paragneisses (Grauert a. Arnold, 1968).

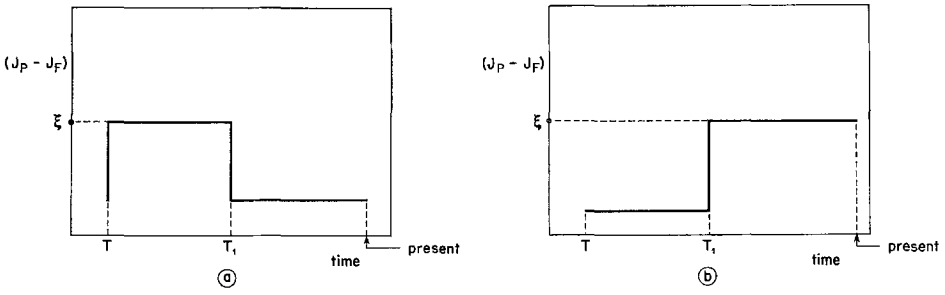

Fig. 9. Multistage continuous loss model. The graph describes changes in $(J_P - J_F)$ during time

b) on the other hand in a given depth range continuous lead loss may be negligible owing to a large activation energy, whereas surface conditions such as weathering may cause continuous losses of lead, uranium and/or thorium between T_1 and the present time (Fig. 9 b).

Calculations are shown in Fig. 10 with $T = 2700$ m. y. and $T_1 = 1000$ m. y. Note that in every case $T_1^* \neq T_1$.

It can be easily shown that any curve of this type can fit the results from the Alps.

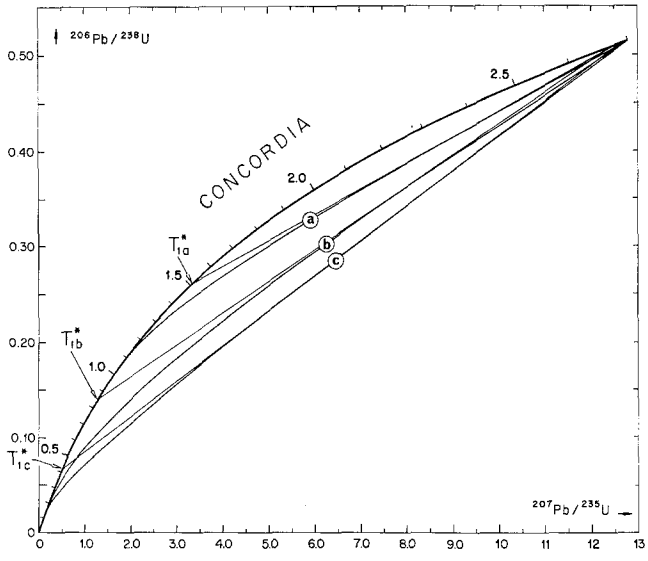

Fig. 10a—c. Discordia plot of the multistage continuous loss model. $T = 2700$ m. y., $T_1 = 1000$ m. y. a Continuous loss between T and T_1. b Continuous loss between T and 0 (Ulrych model). c Continuous loss between T_1 and 0. Note the differencies between the T_1* and T_1

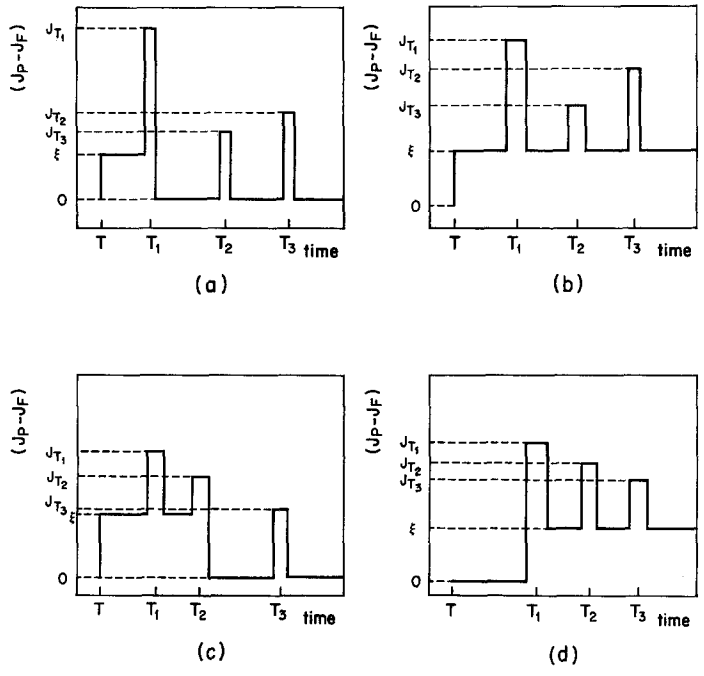

Fig. 11. Multistage continuous + multiepisodic loss model. The diagrams show the variations of the parameter $(J_P - J_F)$ during time, with episodic losses superimposed on continuous losses

3.4. Multistage Continuous + Multiepisodic Loss Model (MC + ME) These models are combinations of the two preceding ones. Four cases will be considered. The assumptions of these models are described graphically in Fig. 11.

Geologically these models may represent combinations of tectono-metamorphic episodic events, such as nappe formation, uplift, folding and faulting and continuous Pb loss as a result of exposure to elevated temperature or as a result of diaphtoresis and weathering processes.

Several discordias corresponding to plausible geological conditions have been calculated (Fig. 12, 13).

With this model we can only explain the results of zircons from the Alps, if we admit a slight influence of the continuous loss. For the whole region, except the Penninic zone, the values of φ and φ' are relatively large, indicating the predominant influence of the Hercynian and the Pre-Hercynian events as compared to the Alpine event.

For all models we find that:

a) the lower intercept T_1* of the extrapolated straight line part of the discordia with the concordia will usually differ from T_1, T_2, or T_3;

b) the upper intercept extrapolated from the lower part of the discordia does not give a primary age T, and that;

c) in the lower part of the diagram the discordias and the concordia are indistinguishable at one or more points, however, these points are generally different from T_1, T_2 and T_3. In other words, concordant U-Pb ages in the part of the diagram do not necessarily indicate a "true" mineral age.

3.5. Conclusions from the Model Calculations.

The zircon data from the Alps are best explained by multiepisodic discordia curves with different φ' and φ values, which satisfy the array of data points for various regions. (Fig. 8). In general, the concordia intercepts obtained by extrapolation of the experimentally determined discordias, do not correspond to T_1, T_2, T_3 or T. Only qualitative limitations of these values can be deduced.

4. Discussion

The first part of the discussion of the zircon data from the Alps deals with the geological significance of the multi-episodic loss model. Then the Precambrian cases of North America and the associated Th-Pb relationships are interpreted Finally the mechanism of lead loss in zircons will be discussed.

4.1. Geological History and the U—Pb Zircon Age Pattern from the Alps.

4.1.1. Preliminary Observations.

Two examples shall illustrate the relations between the observed U-Pb discordia and the geological history.

a) Zircon suites were separated from samples CEN 1 and 2 FM 5, located 200 m apart from one another. One may reasonable assume that the two samples had the same geological history. If our assumption is true that the shape of the discordia is related to the geological history, then the two suites must define the same discordia. The results clearly support our assumption (Fig. 2a).

b) To the west in the Southern Alps, i. e. in the Ivrea zone, the age patterns of samples STRO 2, STRO 3 and ANZ 1 reflect an event 300 m.y. ago (Fig. 2b).

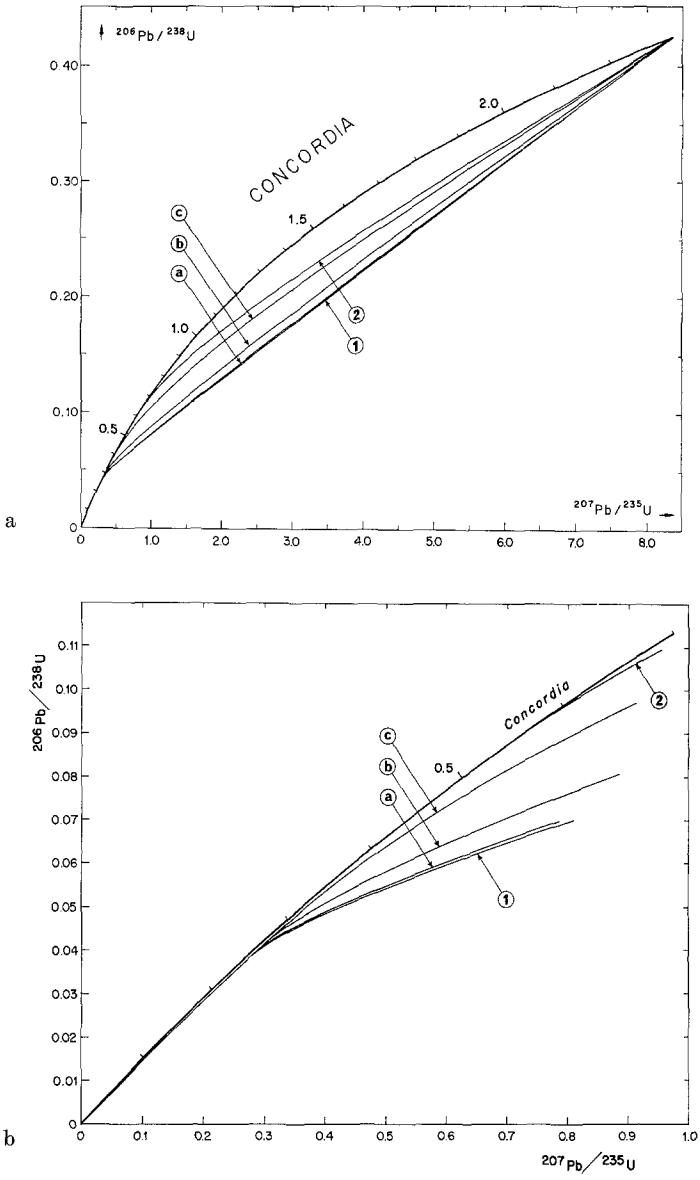

Fig. 12. a Multistage continuous + multiepisodic discordias (model a of Fig. 11) with a continuous loss between T and T_1. For curves *a*, *b* and *c*: $T = 2300$ m. y., $T_1 = 500$ m. y., $T_2 = 300$ m. y., $T_3 = 30$ m. y., $\varphi' = 20$, $\varphi = 20$. The shape of the curves is determined by $A = K_{T_3} \Delta_3 \lambda_8$, curve *a*) $A = 0.1$, curve *b*) $A = 0.01$, curve *c*) $A = 0.001$. 1 and 2 are reference discordias corresponding to the multi-episodic discordia with the same T, T_1, T_2, T_3, φ' and φ and the multistage continuous loss model with a continuous loss between T and T_1. b The figure shows the enlarged bottom part of Fig. 12a

Therefore the zircon history in this area is complicated by the superposition of a strong Hercynian event upon a pre-Hercynian one. Yet the U-Pb zircon ages define a very regular and predictable discordia curve which intersects the con-

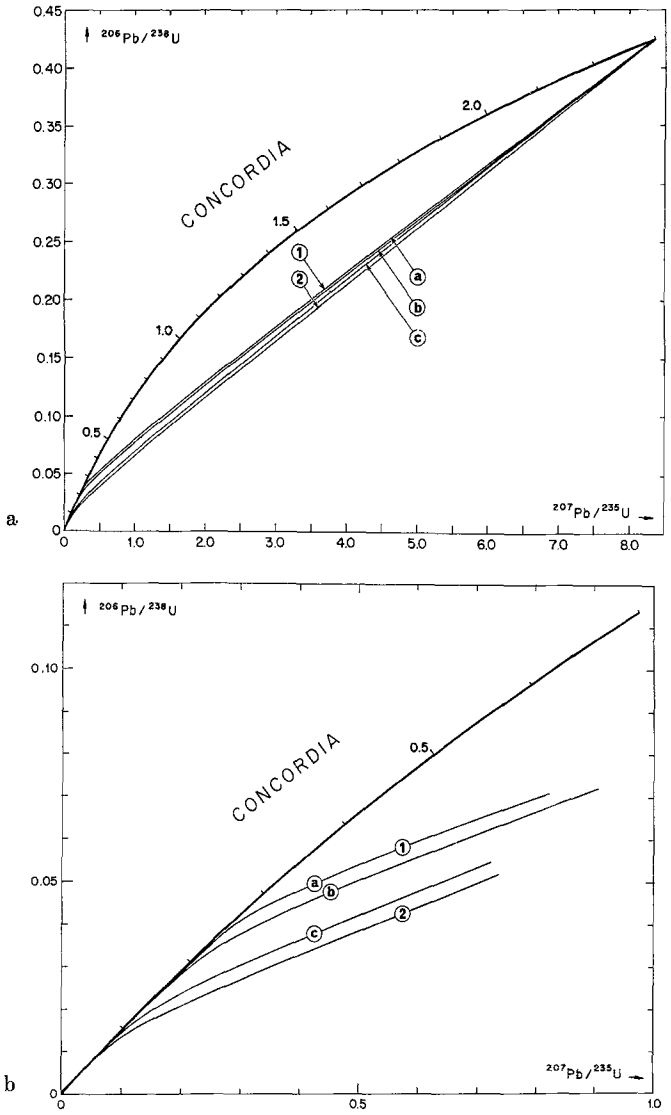

Fig. 13. a Multistage continuous + multiepisodic discordias (model *d* of Fig. 11) with a continuous loss between T_1 and 0. $T = 2300$ m. y., $T_1 = 500$ m. y., $T_2 = 300$ m. y., $T_3 = 30$ m. y.. $\varphi' = 20$, $\varphi = 20$, $A = K_{T_3} \Delta_3 \lambda_8$. The curves *a*), *b*) and *c*) correspond to $A = 0.1$, $A = 0.01$, and $A = 0.001$ respectively. The curves 1 and 2 are reference discordias of 1), the multiepisodic model with the same T, T_1, T_2, φ' and φ and 2) the continuous multistage model with a continuous loss between T_1 and 0, b The figure shows the enlarged bottom part of Fig. 13a

cordia at about 300 m. y. Increasing the values of

$$\varphi = \frac{K_{T_2} \Delta_2}{K_{T_3} \Delta_3}$$

similar curves can be calculated for the discordias given by samples CAS 1 and STRO 1.

Multiepisodic events are clearly evident in the Alps.

Tentatively one can estimate the intensities of the events in the respective areas. Such a study is based on several assumptions.

a) There exists a relation between the efficiency parameter as defined above, and the intensity of a geological event. The relation is, however not simple. Koeppel and Gruenenfelder (1971) showed that detrital paragneiss zircons of the Southern Alps recrystallized under amphibolite facies conditions while retaining a significant part of the accumulated radiogenic lead. Because of annealing of the crystal lattice, a subsequent event will cause a serious disturbance of the U-Pb system only if it is of significantly higher intensity than the previous one, or if the time span between the two events was large enough to enable the radiation to damage the lattice sufficiently.

b) Furthermore we assume that the times T_1, T_2 and T_3 obtain for the entire central Alps. T may vary for different paragneiss zircon suites. One may reasonably assume that it corresponds to one of the known Precambrian events (1.0, 1.3, 1.7, 2.0, 2.3, 2.6 b. y.). Hence, paragneiss zircons of a given sample are treated as if they were a cogenetic suite, although Pidgeon *et al.* (1970) proposed an entirely different explanation that treated the zircon suites as a mixed population with different primary ages.

c) We assume that T_2 and T_3 can be estimated by using the mineral Rb-Sr age results obtained by Jaeger *et al.* (1967) and Hunziker (1970). We agree with Jaeger that orogenies are complex thermal-timing processes, nevertheless we shall use mean values of 300 m. y. for T_2 and 30 m. y. for T_3.

d) The values of T_1 and T can be estimated by means of a best fit between the calculated and observed curves using a programming computer process with a Calcomp plotter.

Since we do not know the number of pre-Hercynian orogenies, this approach will have to be changed if new evidence pertinent to this question is found. For the present time we assume that the pre-Hercynian event T_1 is unique and the same for all investigated areas.

4.1.2. Results

The best fit between calculated multiepisodic and experimentally observed discordias indicates a minimum age of 520 m. y. and a maximum age of 580 m. y. for T_1. The episodic event T_1 may correlate to the Cadomian phase of the Assyntic orogeny known to occur in the Pyrenees (Vitrac and Allègre, 1971) as well as in the Danubian massive of the Carpathians (Gruenenfelder *et al.*, in press). This best fit does not necessarily require the existence of an event 450 m. y. ago. However, recognition of 2 pre-Hercynian events within the central Alps, i. e. $T_1 = 520 - 580$ m.y. and $T_2 = 450$ m. y. is possible.

In areas where the Alpine event is important (Penninic region), the U-Pb age patterns point to a recent lead loss (Fig. 4), however the degree of discordancy is not directly related to the metamorphic grade of the Alpine orogeny. The pattern depends, as shown by the model equation, on the prealpine history as well as on the inherent heterogenities of the zircon. We therefore believe to demonstrate only on a large scale a correlation between the intensity of the Alpine orogeny and

the degree of zircon U-Pb discordancy. This observation justifies studying the regional variation of φ and φ'. The shape of the curves for different pairs of values φ and φ' is shown in Fig. 7.

The mineralogical differences observed between the ortho- and paragneiss zircons indicate that the paragneiss zircons are inherited (Koeppel and Gruenenfelder, 1971). According to assumption b) T represents the age of the source for this type of rocks.

Two cases are considered for T:

a) T is unique for the central Alps and is approximately 2500–2600 m. y.

b) At least two values are considered for T, namely 2000 m. y. and 2500–2600 m. y. (Fig. 8). Any zircon mixtures, as proposed by Pidgeon *et al.* (1970), with an apparent T between 2000 and 2600 m. y. will satisfy the model.

4.1.3. Geographic Variation of φ and φ'

4.1.3.1. T is unique and 2500–2600 m. y.

St. Gotthard: The Rb-Sr mineral ages vary between 16 m. y. (Jaeger, 1967) and 275 m. y. (Arnold, 1970). Therefore we may generalize and state that the Alpine event was in this area of medium intensity. The numerical calculations indicate that the influence of the 550 m. y. event on the U-Pb system in zircons is far superior to that of the Hercynian event, which is characterized by the intrusion of granites. The influence of the Hercynian event is comparable to that of the Alpine event ($\varphi \sim 1$, $\varphi'/\varphi \gg 1$).

Austro-Alpine Silvretta Nappe: The Alpine disturbance is weak, Rb-Sr mineral ages are Hercynian (Grauert, 1966). The Hercynian phase is less important, than the 550 m. y. event ($\varphi > 1$, $\varphi'/\varphi > 1$).

Penninic Region. The Alpine metamorphism reached here its highest grade. It is difficult to estimate φ and φ', because only orthogneiss zircons have so far been analyzed which were formed or completely reset at T_1 or T_2. φ and φ'/φ are variable in this area ($\varphi > 1$).

Southern Alps (Ceneri zone, Fig. 2b): The Alpine metamorphism is very weak. The K-Ar ages of minerals yielded a Hercynian age pattern (McDowell, 1970), but the most intense event seems to have occurred 550 m. y. ago ($\varphi > 1$, $\varphi'/\varphi > 1$) (Hamet and Albarède, 1973).

According to this model the major event affecting the crystalline rocks of the central Swiss Alps occurred 550 m. y. ago (Cadomian orogeny). The influence of the Alpine orogeny is clearly observed in the Penninic region. This view is an agreement with the petrographic observations, that outside the central Penninic zone the effects of the Alpine metamorphism are of retrograde nature (E. Niggli, 1970). The zircon populations discussed in this paper show no evidence for new zircon growth during the Alpine metamorphism, a process that normally has been found, to occur in anatexites (Grauert and Arnold, 1968; Koeppel and Gruenenfelder 1971; Steiger *et al.*, 1972; Gebauer, personal communication).

4.1.3.2. Assumption of Two Discrete Values for T

The best fit for the experimentally determined points (Fig. 8) is calculated by using two values for T, namely 2000 m. y. and 2500–2600 m. y. and constant

values of φ and φ' (respectively 20 and 200) for areas where paragneiss zircons have been analysed. In this hypothesis we therefore assume two source areas for all detrital zircons in paragneisses of the central Alps. Note the fact that again the first event (550 m. y.) is the most intense one.

Further work will show whether regional variations with respect to the source areas can be found and whether they conform to the geochronology of the European Precambrian.

4.2. Zircon U-Pb Age Patterns and Dating of Basement Uplift

The most important results of Steiger and Wasserburg (1969) and Naylor *et al.* (1970) are the relations between the geological history of different Precambrian granitic plutons and the U-Pb zircon age patterns. Using the calculated models, one may reexamine some problems of the Precambrian.

A hypothetical history of a granite may be the following:

1) Crystallisation at time T.

2) Between T and T_1 the granite remains at depth, the zircons behaving as closed systems with respect to uranium and lead.

3) At T_1 the granite is uplifted and subjected to secular alterations.

4) Between T_1 and the present the zircon U-Th-Pb systems are partially open.

The equations for such a history are given in model M-C (Fig. 9b, 10) where the relative positions of T and T_1 define the shape of the discordia. For the boundary cases

a) $T_1 \cong T$, i. e. the time of uplift shortly follows the time of rock formation, the discordia corresponds to a continuous lead loss curve such as proposed by Tilton (1960), and Wasserburg (1963), and

b) $T_1 \ll T$, the shape of the discordia corresponds approximately to the case of a monoepisodic event, however $T_1^* \neq T_1$.

A variation in the time of basement uplift can explain the observed differences in the zircon age pattern of the Precambrian of North-America, which are interpreted by different authors as a result of either an episodic or a continuous lead loss (e. g. Goldich *et al.*, 1970). In the Alps the time of the main basement uplift is recent and the episodic events dominate such that the continuous loss is negligible. In the Precambrian shield areas, however, continuous Pb loss should be more pronounced.

With this model in mind one can reevaluate the results given by Steiger and Wasserburg (1969) on zircons from several coeval granites.

The Quebec case history is characterized by the absence of episodic events after 2700 m. y. Thus we can assume that the basement uplift occurred 2600 m. y. ago, and that the continuous lead loss lasted therefore from then on to the present (Fig. 14).

In the Wyoming case history some small episodic events are detected by the Rb-Sr method (Naylor *et al.*, 1970). We can assume that the basement uplift occurred only at Laramide or Nevadian time, i. e. 60–150 m. y. ago. At this time, an episodic event possibly occurred. The zircon U-Pb age results can be quantitatively explained by the model of type (MC + ME) with:

$$J_{T_1} = J_{T_2} = 0, \quad T_3 = 150 \text{ m. y.} \quad \text{(Fig. 15).}$$

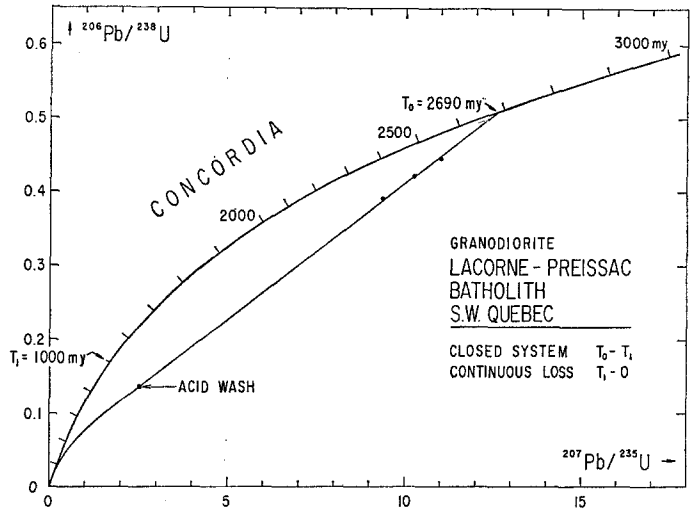

Fig. 14. Lacorne Preissac zircon data (Steiger and Wasserburg, 1969) The curve is calculated according to our model and quoted parameters

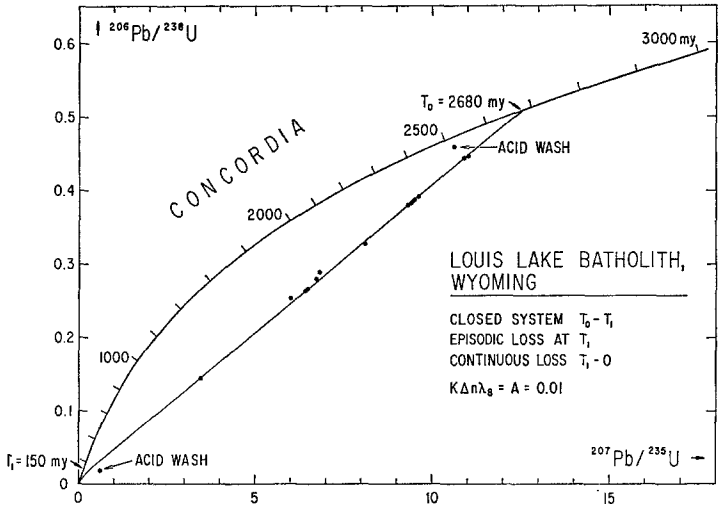

Fig. 15. Louis Lake batholith (Wyoming) zircon data (Naylor *et al.*, 1970). The curve is calculated according to our model and quoted parameters

The contrasting cases illustrate the different zircon behaviour in Precambrian shields uplifted very early in their history, or uplifted only during recent times as is the case in the western United States.

The Timigami lake granite has a more complicated history. At least two episodic events are known in this area after 2700 m. y. The one at 1000 m. y. is well known, however, the first at 1700 m. y. is probably more important (Krogh and Davis, 1971) (Fig. 16).

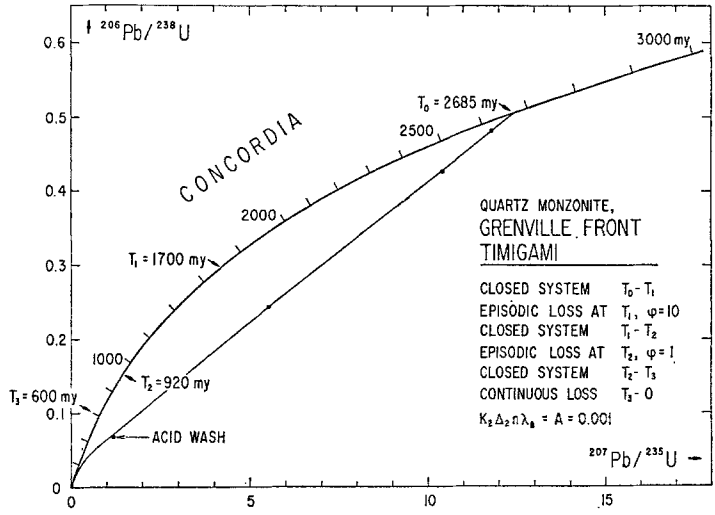

Fig. 16. Timigami zircon data (Steiger and Wasserburg, 1969). The curve is calculated according to our model and quoted parameters

Two episodic events appear to be superimposed upon a continuous Pb loss. It must be pointed out that in spite of this complication, the U-Pb zircon data points exhibit a smooth pattern when plotted on a U-Pb evolution diagram.

Assuming the possibility of a basement uplift 600 m. y. ago, a discordia can be calculated which agrees reasonably well with the observed age pattern. The superposition of episodic events at 1700 and 1000 m. y. does not significantly change the shape of the calculated curve as long as the two events are of minor importance (Fig. 16).

The data suggest that the zircons responded to the uplift of the basement by a continuous Pb loss. The model therefore offers an attractive way of interpreting the Precambrian U-Pb zircon age results, as indicating the approximate time of a basement uplift.

Thus, a general review of the zircon age patterns permits one to distinguish two areas:

a) Shield areas where the basement uplift occurred shortly after its consolidation, and

b) areas where the uplift occurred long after the basement was formed.

These areas may be further subdivided: In the western United States the basement uplift was not accompanied by important episodic effects as is seen from the K-Ar and Rb-Sr mineral ages (Damon, 1968). In the eastern part of the United States, on the other hand, the uplift of the basement is complicated by multiepisodic recycling of the rocks. Therefore the extrapolated T_1^* is grossly different from any particular event, as Tilton (1960) pointed out. The K-Ar and Rb-Sr ages do not contribute any information pertinent to T of the basement (Tilton *et al.*, 1958).

5. $^{208}Pb/^{232}Th$—$^{207}Pb/^{235}U$ Diagram

It is evident that the pattern of data points must be more complex, because uranium and thorium behave chemically different. We will treat quantitatively only those models which apparently fit the observed age patterns.

5.1. Two Episodic Event Model (ME)

Using the same notations as above we obtain:

$$r_{\lambda_5} = (e^{\lambda_5 T_2} - 1) + R_2(e^{\lambda_5 T_1} - e^{\lambda_5 T_2}) + R_2^{(\varphi+1)}(e^{\lambda_5 T} - e^{\lambda_5 T_1}),$$

$$r_{\lambda_2} = (e^{\lambda_2 T_2} - 1) + R_2'(^{\lambda_2 T_1} - e^{\lambda_2 T_2}) + R_2'^{(\varphi^*+1)}(e^{\lambda_2 T} - e^{\lambda_2 T_1}),$$

$$R_2 = e^{K_{T_2}(J_P - J_F)\Delta_2},$$

$$R_2' = e^{K'_{T_2}(J'_P - J_F)\Delta_2}.$$

where K'_{T_2} and J'_P correspond to the Th-Pb system.

$$\varphi_{^{238}U} = \varphi = \frac{K_{T_1}\Delta_1}{K_{T_2}\Delta_2}; \quad \varphi_{^{232}Th} = \varphi^* = \frac{K'_{T_1}\Delta_1}{K'_{T_2}\Delta_2}.$$

Both r_{λ_5} and r_{λ_2} equations for a zircon population of the same age are related by the four parameters R_2, R_2', φ and φ^*. If these four parameters are independently variable, the data points of different zircon fractions will scatter in a r_{λ_5}, r_{λ_2} diagram.

Restricting the degree of freedom, we use (similar to Steiger and Wasserburg, 1966) $R'_2 = R_2^{k_2}$ and $R'_1 = R_1^{k_1}$. It follows that $\varphi^*/\varphi = k_1/k_2$. In this case it is assumed that for a given zircon population k_1, k_2 and R_1 are constants, and that therefore only R_2 is a parameter which varies between 0 and 1. Allègre (1965) has pointed out that k_1 or k_2 can be >1 or <1. The discordia is then a curve, which has been calculated for two interesting cases:

a) $k_1 = k_2$, i. e. the two episodic events are of the same nature with respect to U-Th fractionations (Fig. 17a, b) and

b) $k_1 \neq k_2$, i. e. the two episodic events differ with respect to U-Th fractionations (Fig. 17c, d).

The discordias are therefore calculated with two different values for k [the slope of the experimental discordia of the U-Th-Pb diagram is obtained by multiplying the slope of the line, determined by T and T_1, by k (Steiger and Wasserburg, 1966)]. Thus, two types of k parameters can be calculated.

Taking k_1 for one and k_2 for the other model and using different values of φ yields different discordias, which are more complex than the corresponding discordias in the U-Pb evolution diagram.

Such complex curves are experimentally obtained only if the above relations are satisfied, otherwise the data points will scatter. There are only few experimental results which do not show any regularities in the U-Th-Pb diagram. The intercepts obtained by the "best experimental line" and the concordia are without geological significance and in general give values for T, T_1 or T_2 that are different from those obtained in the U-Pb diagram.

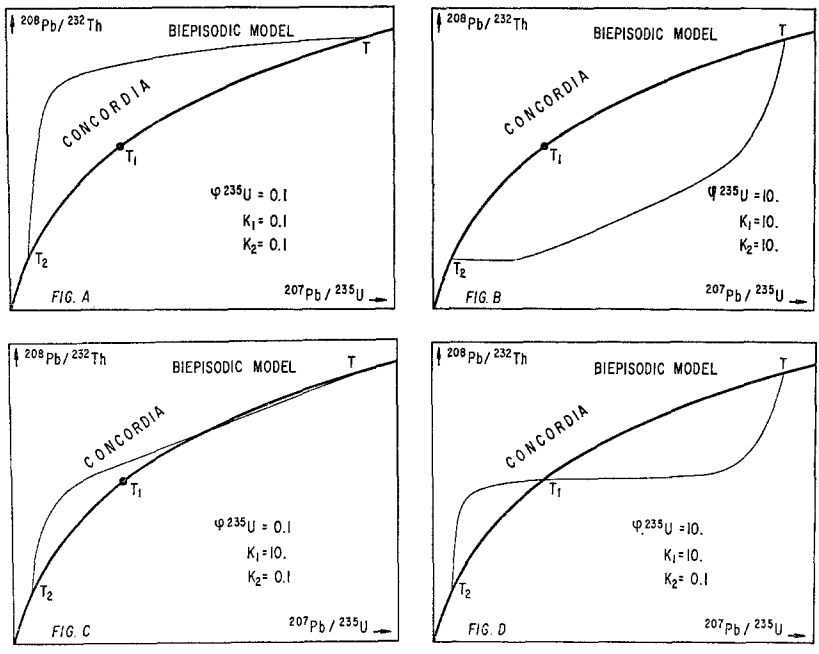

Fig. 17 a–d. $^{208}Pb/^{232}Th$-$^{207}Pb/^{235}U$ diagrams showing multiepisodic discordias. The parameters are indicated on the diagrams

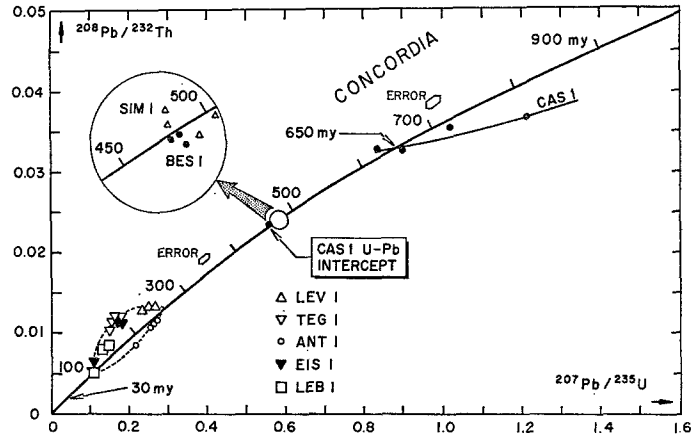

Fig. 18. $^{208}Pb/^{232}Th$-$^{207}Pb/^{235}U$ diagram showing data points of samples from the Penninic area and the Southern Alps (CAS 1). The lower intercepts of the U-Pb arrays (Fig. 2a, 4a, 4b) are clearly different from the U-Th-Pb intercepts. The curves drawn are only boundary curves

5.2. Continuous Loss during Discrete Stages (MC)

For model MC_a

$$r_{\lambda_5} = \frac{\lambda_5 e^{\lambda_5 T_1}}{\lambda_5 + \xi} (e^{(\lambda_5 + \xi)(T - T_1)} - 1) + (e^{\lambda_5 T_1} - 1)$$

$$r_{\lambda_2} = \frac{\lambda_2 e^{\lambda_2 T_1}}{\lambda_2 + \xi'} (e^{(\lambda_2 + \xi')(T - T_1)} - 1) + (e^{\lambda_2 T_1} - 1).$$

(MC_b could be treated in the same manner.)

Assuming a relation between ξ and ξ', e. g. $\xi/\xi' = \Theta$ one can calculate the discordia of the Th-U-Pb diagram. With a resonable value Θ the discordia is a straight line in the upper part. The line intercepts the concordia at T (initial age), the slopes depending on the values of Θ.

5.3. Multiepisodic-Continuous Loss + Multiepisodic Model (MC + ME).

One discordia calculation shows the principles: Two episodic loss events are combined with a continuous Pb-loss during the entire history of the zircon. The equations are:

$$r_{\lambda_5} = \frac{\lambda_5}{\lambda_5+\xi}\left\{(e^{(\lambda_5+\xi)T_2}-1)+e^{K_{T_2}\Delta_2\xi}(e^{(\lambda_5+\xi)T_1}- e^{(\lambda_5+\xi)T_2}) + e^{K_{T_2}\Delta_2\xi(\varphi+1)}(e^{(\lambda_5+\xi)T}-e^{(\lambda_5+\xi)T_1})\right\}$$

$$r_{\lambda_5} = \frac{\lambda_2}{\lambda_2+\xi'}\left\{(e^{(\lambda_2+\xi')T_2}-1)+e^{K_{T_2}\Delta_2\xi'}(e^{(\lambda_2+\xi')T_1} -e^{(\lambda_2+\xi')T_2})+e^{K'_{T_2}\Delta_2\xi'(\varphi^*+1)}(e^{(\lambda_2+\xi')T}-e^{(\lambda_2+\xi')T_1})\right\}$$

The solution depends on 6 parameters: K_{T_2}, K'_{T_2}, ξ, ξ', φ, and φ^*, and a discordia is defined only by assuming particular conditions. For one case assume

$$\frac{K_{T_2}}{K'_{T_2}} = D, \qquad \frac{\varphi}{\varphi^*} = \tau, \qquad \frac{\xi'}{\xi} = \mu.$$

D, τ and μ being constant for one zircon population a discordia can be calculated.

5.4. Variation of the Th/U Ratio with the Degree of Discordancies

Steiger and Wasserburg (1966) have demonstrated that in a two phase episodic model the Th/U ratio varies monotonically with the degree of discordance. If the discordia lies above the concordia, the Th/U ratio decreases with the degree of discordancy. If the discordia lies below the concordia, the opposite correlation is observed. Steiger and Wasserburg (1969) presented two cases that contradict their theory:

a) In the case of the Lacorne granite the zircon population contained a "leaching phase", which constitutes according to the views of Steiger-Wasserburg one end member of the two phase systems, having a Th/U ratio that contradicts the prediction.

b) In the case of Timigami zircons the variations of the Th/U ratios contradict the theory.

Therefore it is of interest to calculate the Th/U ratios as a function of the degree of discordancies. For two episodic cases one can write:

$$(\mathrm{Th/U})_{\text{discordant fraction}} = (\mathrm{Th/U})_{\text{concordant fraction}}\, R_2^{[(k_2+1)+(k_1+1)]}$$

k_1, k_2 and φ being kept constant; the Th/U ratio varies with R_2 quite monotonically with the degree of discordancies; however, in contrast to the two-phase Steiger-Wasserburg model, variations of the Th/U ratio with the degree of discordancy depend on k_2, k_1 and φ. Therefore the Th/U ratios may increase or decrease independently of the position of the discordia with respect to the concordia.

5.5. Conclusions from the U-Th-Pb Diagrams.

A complicated geological history of the zircons destroys the smooth pattern of data points in the U-Th-Pb diagram in agreement with both the theoretical calculations and the observed arrays of data points. The geologically complex case of the Timigami granite, studied by Steiger and Wasserburg (1969), yielded complex data patterns and opposing correlations of the Th/U ratio with the degree of discordancy.

If the geological history is simpler, as for instance in shield areas, the experimentally determined U-Th-Pb age patterns are simple and the Th/U ratio varies monotonically in the same direction.

The U-Th-Pb diagram offers sensitive means to evaluate the complex geological character of an area. The Grenville case, studied by Steiger and Wasserburg (1969) yielded a complex pattern and therefore supports Krogh's hypothesis of two episodic events at 1000 and 1700 m. y. The few measurements of paragneiss zircons from the Alps also exhibit complex pattern of data points (Fig. 18).

6. U-Th-Pb Loss Mechanism and Zircon Discordancy

As we have pointed out in the previous section, some observations are in contradiction with the Steiger-Wasserburg (1966) model regarding the zircons as two phase mixtures. Even more important contradictions are:

a) The variation of the Th/U ratios, their relation to the degree of discordancy, and the observed scattered patterns of data points in a U-Th-Pb diagram.

b) The observation made by Catanzaro (1963) that some extrapolated lower intercepts T_1* cannot be explained by any continuous diffusion mechanism.

c) Grauert and Arnold (1968) show a regularily curved U-Pb-discordia which cannot be interpreted as a two phase mixing line.

Nevertheless, some arguments, particularily with reference to the results from washing experiments, given by Steiger and Wasserburg (1969), strongly argue for two phase systems to occur in several instances. For a general explanation of this phenomenon, we adopt the following model:

1) Zircons are single phases and closed systems, provided they remain in plutonic environments, at depth.

2) If the rock is uplifted, and stressed, unmixing of zircons may occur, resulting in a two or multiple phase system. The U-Th-Pb system phases may be almost open, whereas in other phases it is virtually closed.

3) During the unmixing process chemical fractionations and losses of U, Th, and Pb may occur (Gruenenfelder, in prep.).

In the case of the Alps the uplift is very recent and the problem of continuous Pb loss in one of the phases is usually negligible. Therefore most zircons may be treated approximately as a one phase system.

In the Canadian shield, however, where the uplift occurred shortly after the consolidation of the basement, an unmixing process must be of importance with respect to a continuous lead loss. The U-Th-Pb age patterns are sometimes very complex, because superimposed upon Th/U fractionations are natural leaching processes and episodic events.

4) Hart *et al.* (1968) show that in the case of a contact metamorphism the activation energy of lead in zircons is much higher than of ^{40}Ar in biotite, whereas on the other hand cases are known, where concordant K-Ar and Rb-Sr ages of micas are higher than the apparent U-Th-Pb ages. This paradox may be solved by assuming that after unmixing there are two activation energies for Pb. For one phase it is high, whereas for the other phase it is low, particularily in a water bearing environment.

The existence of two phases, one of which having high U and Th concentrations and being readily soluble, would account for the observation that detrital paragneiss zircons hardly ever contain more than 1000 ppm of U, because the phase rich in U and Th would be preferentially destroyed by chemical and mechanical action such as weathering and sedimentation of the zircons.

This model is furthermore supported by

a) the observations made by Steiger and Wasserburg (1969) in their leaching experiment,

b) the studies by Stern *et al.* (1966) and Kulp (1957),

c) the observations on the unmixing of zircons by Gruenenfelder *et al.* (1967 and in prep.),

d) by the X-ray and electron microprobe investigation on zircons by Koeppel and Gruenenfelder (1971) and Koeppel and Sommerauer (in press).

By adopting this point of view, several apparent contradictions as well as some remarkable differences between ortho- and paragneiss zircons can be explained.

7. Orthogneisses and Paragneisses

It has been already pointed out that the data points of orthogneiss zircons from the central Alps lie close to the concordia, whereas the data points from paragneiss zircons are strongly discordant.

Petrographic evidence often suggests that the orthogneisses are of anatectic origin. Detailed studies on the zircons reveal that they were on the whole newly formed during the anatexis, but that they usually have retained a small amount of approximately 1% of an old radiogenic lead component. Thus a small part of the original detrital zircon suite may survive an anatectic event.

The near-concordant position of orthogneiss zircon data in the U-Pb diagram is predicted by the calculations. The near concordancy, respectively the extreme discordancy as compared to the data of the paragneiss zircons, can be partially explained by an uranium gain. The lattice is, in contrast to that of the paragneiss zircons, not annealed, showing a pronounced domain structure. Thus any subsequent event will have a stronger influence on their U-Th-Pb systems than upon the paragneiss zircon suites.

Summary

The zircon data points of populations separated into fractions of different grain sizes and magnetic susceptibilities (Silver and Deutsch, 1963) from polymetamorphic rocks exhibit on a U-Pb evolution diagram regular arrays. Such a behaviour can only be explained by assuming that within one suite repeated lead losses (or U gains) of the different fractions are systematically related to each other.

By using mathematical relationships for a first order kinetic process the times of disturbances and the relative intensities of the events causing Pb-losses can be evaluated.

Three types of models are developed:

1) a multi-episodic loss model,

2) a multi-stage continuous loss model,

3) a multi-stage continuous + multi-episodic loss model.

The rates of loss during the subsequent events or periods of continuous diffusion are related by an efficiency parameter which is a relative measure of the intensities and durations of the events, and thereby defines the shape of the discordia curves.

In deciding which of the models applies best to the data of samples from the Alps one has to consider the results of field observations and of geochronological investigations using other methods which for the purpose of calculating the models may be simplified to 3 events: T_1 a pre-Hercynian event, T_2 the Hercynian event at 300 m. y. and T_3 the Alpine event at 30 m. y. T and T_1 can then be estimated from a best fit between the calculated and observed discordias.

In this approach we treat the paragneiss zircon suites as quasi cogenetic.

The fit between the calculated and observed discordias indicates a T_1 of 520–580 m. y. which would correspond to a Cadomian phase of the Assyntic orogeny and a T of 2500–2600 m. y. Other models may be calculated using two values for T (2000 m. y. and 2500–2600 m. y.).

The calculations show that a continuous lead loss superimposed on the episodic losses can only be of minor importance. Furthermore the zircon data do not necessarily indicate the existence of a Caledonian event.

In areas were paragneiss zircons have been analysed the shape of the discordia indicates that the Cadomian event was the most intense of the three events. Only in the Ivrea zone of the Southern Alps do we note an equally strong or stronger influence of the Hercynian event.

In the Penninic region only zircons from orthogneisses have been analysed. They probably were formed at T_1 or T_2 and/or completely reset under anatetic conditions.

Only a rough estimate of the relative intensities of the events can be made because the behaviour of the U-Th-Pb systems of a zircon population depends also on inherent properties of the crystals such as the trace element, including the water contents and the manner of incorporation of the trace elements into the crystals. Furthermore the crystal lattice of the zircons may be annealed during an early episode and subsequent events of similar intensities affect the U-Th-Pb less drastically than the first.

An examination of zircon data from North America shows that some fit multistage continuous loss models or multistage continuous + multiepisodic loss models with only a minor influence of the episodic loss. Assuming closed U-Pb system behaviour of the zircons at depths and opening of the systems upon uplift, because of either unmixing effects or exposure to weathering, these models offer the possibility of dating periods of uplift of the basement.

Zircon populations with complex histories may yield on a $^{206}Pb/^{238}U$-$^{207}Pb/^{235}U$ diagram arrays of data points ressembling that of a population with a simple

Table 1. Analytical zircon data

Sample grain size (microns) and magnetic susceptibility at 1.6 A	U content (ppm)	Th content (ppm)	Rad.Pb content (ppm)	Observed ratios			Apparent ages in m.y.			
				$^{206}Pb/^{204}Pb$	$^{207}Pb/^{204}Pb$	$^{208}Pb/^{204}Pb$	$^{206}Pb/^{238}U$	$^{207}Pb/^{235}U$	$^{207}Pb/^{206}Pb$	$^{208}Pb/^{232}Th$
MATO 1										
+150 —	415	—	20.2	246.1	27.63	59.80	312	321	388	—
150— 75 n.m.	458	—	22.2	484.5	40.16	85.89	309	315	354	—
53— 42 n.m.	669	—	30.8	1496	93.35	203.7	292	297	334	—
— 53 m.	789	—	35.1	887.2	60.92	140.1	281	285	317	—
SIM 1										
+75 n.m.	415	86.4	30.5	1138	84.34	116.2	473	510	677	502
75—53 n.m.	419	84.0	30.4	1984	130.7	162.5	472	489	572	469
53—42 n.m.	482	85.0	32.6	2292	147.5	174.1	442	460	548	471
—42 n.m.	507	81.8	34.0	3301	206.0	229.4	439	457	547	492
LEV 1										
+53 n.m.	1826	341	69.2	1843	111.3	154.4	252	259	322	268
53–42 n.m.	1890	393	69.5	2265	132.8	204.6	243	249	309	268
—42 n.m.	2077	451	73.4	3110	176.7	258.4	232	239	303	265
LEV 2										
— n.m.	791	213	28.3	1864	114.2	222.5	231	243	364	265
BRI 1										
75— 50 —	689	—	29.0	962.6	67.9	79.67	283	303	456	—
150— 75 —	—	—	—	1242	82.6	103.1	—	—	422	—
+150 —	861	—	35.0	204.7	26.03	46.06	272	301	526	—
TEG 1										
+75 n.m.	1433	222	33.5	416.5	36.09	67.20	155	165	305	232
75—53 n.m.	1247	184	27.0	611.8	46.00	83.36	144	152	283	233
53—42 n.m.	1425	195	28.7	918.5	61.91	106.0	133	142	285	229
—53 m.	1745	252	32.4	657.2	48.41	86.01	123	132	287	200

VER 1										
+65 n.m.	1993	470	51.8	239.8	26.95	59.44	168	177	288	222
−65 m.	3255	654	64.8	116.1	20.47	45.57	131	140	294	174
ANT 1										
+100 n.m.	818	304	28.3	1234	78.41	176.3	221	227	291	209
75− 53 n.m.	970	405	34.4	1926	114.2	282.6	223	229	289	212
42− 30 n.m.	909	399	32.8	1942	115.7	303.2	225	232	303	219
− 42 m.	1146	561	33.4	1307	82.06	219.8	182	190	286	163
Ant 2										
+53 n.m.	1362	431	38.8	329.4	31.65	75.64	181	191	324	218
— m.	1540	524	40.8	318.7	30.96	76.41	167	175	276	195
LEB 1										
+65 n.m.	2058	466	42.6	355.9	32.96	68.15	135	145	296	169
−65 n.m.	2464	476	42.00	448.9	37.73	75.11	112	121	297	155
−65 m.	2820	719	40.5	177.6	23.48	51.94	94	101	262	103
MLE 1										
−53 n.m.	2828	647	57.5	726.9	51.06	101.9	133	138	225	166
BES 1										
+75 n.m.	771	253	54.6	853.3	63.15	129.5	446	467	516	438
53−42 n.m.	879	299	62.9	2044	129.8	257.0	448	456	492	452
−42 n.m.	950	338	67.9	3562	215.7	446.0	445	452	487	450
GAT 1										
+100 n.m.	507	245	19.3	372.6	34.48	96.83	231	246	368	248
53− 42 n.m.	759	393	25.8	629.5	47.33	146.7	206	215	316	220
− 42 —	970	537	31.4	470.6	39.12	121.6	194	205	323	201
EIS 1										
+75 n.m.	459	118	11.6	181.0	23.93	56.54	161	173	336	225
53−42 n.m.	838	180	19.5	388.5	34.75	77.16	150	161	317	230
−42 m.	1747	410	23.5	254.7	27.44	63.35	87	94	262	124

Common lead correction: $^{206}Pb/^{204}Pb$: 17.66; $^{207}Pb/^{204}Pb$: 15.26; $^{208}Pb/^{204}Pb$: 37.04.

history. However on a $^{207}Pb/^{235}U$-$^{208}Pb/^{232}Th$ plot the complex history may readily be noticeable because of the chemically different behaviour of U and Th, which may lead to different U-Th fractionations during subsequent events. The resulting arrays yield extrapolated intercepts with the concordia curve that are different from those of the U-Pb diagram and have no geological significance.

Acknowledgements. We wish to thank Y. Bottinga, P. Signer and R. H. Steiger for reading the manuscript and helpful discussion. We also want to thank O. Krebs and W. Wittwer for their efforts in separating the minerals, in the chemistry lab and in the masspectrometric measurements which made it possible to have most of the data ready for the field trip of the Colloquium on the Geochronology of Phanerozoic Orogenic Belts in 1969.

Appendix I

Sequence Calculations of Complex Models

Example I. a system remains closed from T to 0, except for two episodic losses at T_1 and T_2 with respective loss parameters R_1 and R_2. Proceeding step by step, we get:

$$
\begin{aligned}
r(T_1) &= e^{\lambda(T-T_1)}-1\\
r(T_1-\Delta_1) &= R_1\{e^{\lambda(T-T_1)}-1\}\\
r(T_2) &= e^{\lambda(T_1-T_2)}-1+R_1\{e^{\lambda(T-T_1)}-1\}\ e^{\lambda(T_1-T_2)}\\
r(T_2-\Delta_2) &= R_2\{e^{\lambda(T_1-T_2)}-1\}+R_1R_2\{e^{\lambda(T-T_2)}-e^{\lambda(T_1-T_2)}\}\\
r\ (\text{present}) &= e^{\lambda T_2}-1+R_2\{e^{\lambda T_1}-e^{\lambda T_2}\}+R_1R_2\{e^{\lambda T}-e^{\lambda T_1}\}\\
&\text{Putting } R_1=R_2^{\varphi}\\
r\ (\text{present}) &= e^{\lambda T_2}-1+R_2\{e^{\lambda T_1}-e^{\lambda T_2}\}+R_2^{(\varphi+1)}\{e^{\lambda T-e^{\lambda T_1}}\}.
\end{aligned}
$$

Example II. a system remains closed from T to T_1, at which time it undergoes an episodic loss (R_1). Continuous loss (ξ) occurs from T_1 to 0.

$$
\begin{aligned}
r(T_1) &= e^{\lambda(T-T_1)}\\
r(T_1-\Delta_1) &= R_1\{e^{\lambda(T-T_1)}-1\}\\
r\ (\text{present}) &= \frac{\lambda}{\lambda+\xi}\{e^{(\lambda+\xi)T_1}-1\}+R_1\{e^{\lambda(T-T_1)}-1\}\ e^{(\lambda+\xi)T_1}.
\end{aligned}
$$

Putting $R_1=\exp(K_1\Delta_1\xi)$: we get a function of the single variable ξ.

The building of the sequence of events by a computer enables us to consider various complex models. Furthermore, this scheme has been enlarged to include diffusion models.

Appendix II

Sample Location and Description

Sample locations, rock types and current petrogenetic interpretations are listed in the following Table 2 as well as the zircon properties that deviate from the following general pattern:

Zircons are pink in colour. The majority of the grains are prismatic and euhedral. The crystal faces of many grains are damaged as if they had been mechanically chipped or possibly corroded (Fig. 19a). Usually few rounded as well as some euhedral isometric grains occur (Fig. 19b) They are interpreted as representing detrital rounded grains that developed during metamorphism new crystal faces (Koeppel and Gruenenfelder, 1971).

The crystals are generally transparent and no optical zoning is visible. Fractions of higher magnetic susceptibility tend to contain more zircons with translucent to opaque domains which are often arranged in zones. Populations with abundant translucent to opaque zircons tend to have higher uranium contents than those with mainly clear transparent zircons. It is noteworthy that the zircons from the Simplon area are generally richer in uranium than those from the central Penninic region. A noticeable exception is sample BES 1 which is very low in uranium similar to sample SIM 1.

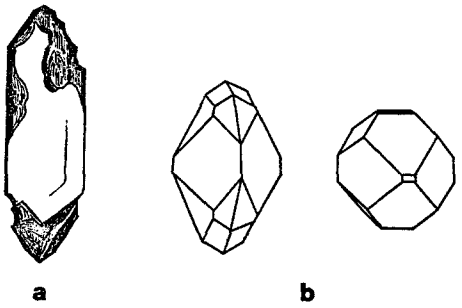

Fig. 19. a Euhedral zircon with chipped or corroded crystal faces. b Euhedral zircons with a short prismatic to isometric habitus which may indicate that the grains were originally rounded but developped new crystal faces during the metamorphism

Table 2 Location and description of samples from the Penninic area

Sample, Mineral constituents	Locality, coordinates, tectonic unit	Petrogenetic interpretation	Zircon characteristics
MATO 1, Matorellogneiss, Qz, alc.-f, plag, bi.	Lago Sambucco, 692.15/147.10, Maggia lobe.	Niggli *et al.* (1936): pre-Triassic intrusive granite, metamorphosed during Alpine orogeny. Guenthert (1954): metamorphosed arkose, granitised during Alpine orogeny.	No rounded or isometric grains. Mainly transparent crystals.
SIM 1, Simanogneiss, Qz, alc-f, plag, bi, ± mu.	Pte. Leginna, Val Blenio, 719.10/138.45, Simano nappe.	Niggli *et al.* (1936): Hercynian granite metamorphosed during Alpine orogeny. Bruggmann (1965): possibly of sedimentary origin.	Grains with translucent domains are rare.
LEV 1, LEV 2, Leventinagneiss Qz, plag, bi, alc-f.	N of Lavorgo, 707.00/145.83, S of Osogna, 719.50/129.80, deepest unit in E Penninic area.	Niggli *et al.* (1936), Casasopra (1939, 1948), Keller (1968): pre-Triassic granite, metamorphosed during Alpine orogeny.	Longprismatic, few with translucent zones or zones rich in inclusions.
BRI 1, Verzascagneiss, Qz, plag, alc-f, mu, bi.	Brione, Valle Verzasca, 703.25/128.25, same locality as Berne standard muscovite and biotite (Jaeger *et al.*, 1963)	Niggli *et al.* (1936): pre-Triassic granite metamorphosed during Alpine orogeny. Wenk (1943): rock granitised during Alpine orogeny.	Small crystals are long-prismatic. Large crystals are short-prismatic to isometric.
TEG 1, banded gneiss, Qz, alc-f, plag, bi.	Tegna, Ponte Brolla, 703.10/115.95, "root zone".	Kobe (1956): alpine migmatite derived from either pre-Alpine crystalline basement or mesozoic sediments.	Colour: Greyish-pink. Often with translucent domains and with over- or outgrowths.
VER 1, Verampiogneiss, Qz, plag, alc-f, little bi and mu.	Valle Antigorio, 668.90/121.80, deepest unit in W Penninic area.	Hunziker (1966): pre-Triassic migmatite, metamorphosed during Alpine orogeny.	Zircons often with translucent domains, some with overgrowth.

Sample, Mineral constituents	Locality, coordinates, tectonis unit	Petrogenetic Interpretation	Zircon caracteristics
ANT 1, ANT 2, Antigoriogneiss, Qz, plag, alc-f, mu, bi, little garnet.	ANT 1: N of Rencio Superiore, Valle Antigorio, 667.75/117.30, ANT 2: E of Gondo, Simplon Road, 654.60/116.43, Antigorio nappe.	Milnes (1965), Hunziker (1966): polymetamorphic gneiss with schollen of biotite-plagioclasegneiss in various stage of assimilation of pre-Triassic age, metamorphosed during Alpine orogeny.	
LEB 1, Lebendungneiss, Qz, plag, alc-f, mu, bi, some garnet.	Alte Kaserne, Simplon Road, 650.40/115.20, Lebendun nappe.	Bearth (1967): post-Hercynian sediment metamorphosed during Alpine orogeny. Milnes (1965 and oral communication): pre-Triassic basement with conglomerate and granitic gneisses.	Colour: Milky-pink, Short-prismatic. Most grains with translucent domains marking a zonality. Opaque grains. No isometric crystals.
MLE 1, Monte Leone-gneiss, Qz, alc-f, plag, bi, mu.	E of Gabi Simplon Road, 647.25/115.05. Monte Leone nappe.	Streckeisen (1967): pre-Triassic granite metamorphosed during Alpine orogeny.	Colour: greyish-pink. Mainly translucent to opaque. No isometric grains.
BES 1, Berisalgneiss, Qz, alc-f, bi, pheng. mu, plag, ep, clz.	Rothwald, Simplon Road, 646.10/125.65, Berisal nappe	Streckeisen (1967): pre-Triassic granite metamorphosed during Alpine orogeny.	Few crystals with translucent domains.
GAT 1, Gantergneiss, Qz, alc-f, green bi, pheng. mu, ep, clz, carbonates.	W of Ganter bridge, Simplon Road, 647.20/127.60, Monte Leone nappe.	Streckeisen (1967): pre-Triassic granite metamorphosed during Alpine orogeny.	Colour: Milky-pink. Many crystals with translucent to opaque domains. Some over- and outgrowths. No isometric grains.
EIS 1, Eistengneiss, Qz, alc-f, pheng, mu.	E of Schallberg, Simplon Road, 646.60/127.55, Monte Leone nappe.	Streckeisen (1967): pre-Triassic granite metamorphosed during Alpine orogeny.	Colour: Milky-pink. Often with translucent to opaque centers. Abundant inclusions of exsolved (?) xenotime.

Qz = quartz, plag = plagioclase, alc-f = alcali-feldspar, bi = biotite, mu = muscovite, pheng. mu = phengitic muscovite, ep = epidote, clz = clinozoisite.

References

Ahrens, L.: The convergent lead ages of the oldest monazites and uraninites. Geochim. Cosmochim. Acta **7**, 294–300 (1955)

Allègre, C. J.: Unpublished report (1965)

Allègre, C. J.: Méthode de discussion géochronologique concordia généralisée. Earth Planet. Sci. Lett. **2**, 57–66 (1967)

Arnold, A.: On the history of the Gotthard massive. (Abstract). Eclogae Geol. Helv. **63**, 29–30 (1970)

Bearth, P.: In: Geologischer Führer der Schweiz, S. 346–348. Basel 1967

Bruggmann, H.: Geologie und Petrographie des südlichen Misox, Dissertation, Universität Zürich, 1965

Cadisch, J.: Geologie der Schweizer Alpen. Basel, 1953

Casasopra, S.: Studio petrografico dello Gneiss granitico Leventina. Schweiz. Mineral. Petrog. Mitt. **19**, 449–708 (1939)

Casasopra, S.: Brevi cenni sulla genesi del granito gneissico Leventina. Schweiz. Mineral. Petrog. Mitt. **28**, 127–139 (1948)

Catanzaro, E. J.: Zircon ages in southwestern Minnesota. J. Geophys. Res. **68**, 2045–2048 (1963)

Catanzaro, E. J., Kulp, J. L.: Discordant zircons from the Little Belt (Montana), Beartooth (Montana) and Santa Catalina (Arizona) Mountains. Geochim. Cosmochim. Acta **28**, 87–124 (1964)

Craig, H.: Zircon lead loss: a kinetic model, Science **159**, 447 (1968)

Damon, P. E.: Potassium-argon dating of igneous and metamorphic rocks with applications to the Basin ranges of Arizona and Sonora. In: Radiometric dating for geologists, eds. Hamilton, E. I. and Farquhar, R. M., p. 1–71. London 1968

Goldich, S. S., Hedge, C. E., Stern, T. W.: Age of the Morton and Montevideo Gneisses and Related Rocks, Southwestern Minnesota. Bull. Geol. Soc. Am. **81**, 3671–3695 (1970)

Grauert, B.: Rb-Sr age determinations on orthogneisses of the Silvretta (Switzerland). Earth Planet. Sci. Lett. **1**, 139–147 (1966)

Grauert, B., Arnold, A.: Deutung diskordanter Zirkonalter der Silvrettadecke und des Gotthardmassivs (Schweizer Alpen). Contr. Mineral. and Petrol. **20**, 34–56 (1968)

Gruenenfelder, M., Hanson, G. N., Brunner, G. O., Eberhard, E.: U-Pb discordance and phase unmixing in zircons. Bull. Geol. Soc. Am. **77**, 1202 (1966)

Gruenenfelder, M., Krebs, O., Soroiu, M., Popescu, G.: Radiometric dating in the southern branch of the Romanian Carpathians: U-Th-Pb and K-Ar ages of the Susita and Tismana granitoids. In press.

Günthert, A.: Beiträge zur Petrographie und Geologie des Maggia-Lappens. Schweiz. Mineral. Petrog. Mitt. **34**, 1–159 (1954)

Hamet, J., Albarède, F.: Rb-Sr geochronology of the Ceneri zone (Southern Alps). Fortschr. Mineral. **50**, Beiheft 3, 80–82 (1973)

Hart, S. R., Davis, G. L., Steiger, R. H., Tilton, G. R.: A comparison of the isotopic mineral age variations and petrologic changes induced by contact metamorphism. In: Radiometric dating for geologists, eds. Hamilton, E. I. and Farquhar, R. M., p. 73–110. London 1968

Hunziker, H. J.: Zur Geologie und Geochemie des Gebietes zwischen Valle Antigorio (Prov. di Novara) und Valli di Campo (Kt. Tessin). Schweiz. Mineral. Petrog. Mitt. **46**, 473–552 (1966)

Hunziker, J. C.: Polymetamorphism in the Monte Rosa, Western Alps. Eclogae Geol. Helv. **63**, 151–161 (1970)

Jäger, E., Niggli, E., Baethge, H.: Two standard minerals, biotite and muscovite, for Rb-Sr and K-Ar age determinations, sample Bern 4 B and Bern 4 M from a gneiss from Brione, Valle Verzasca (Switzerland). Schweiz. Mineral. Petrog. Mitt. **43**, 465–470 (1963)

Jaeger, E., Niggli, E., Wenk, E.: Rb-Sr Altersbestimmungen an Glimmern der Zentralalpen. Beitr. Geol. Karte Schweiz. NF 134 (1967)

Keller, F.: Mineralparagenesen und Geologie der Campo Tencia — Pizzo Forno — Gebirgsgruppe. Beitr. Geol. Karte Schweiz NF 135 (1968)

Kobe, H.: Geologisch-petrographische Untersuchungen in der Tessiner Wurzelzone zwischen Vergeletto-Onsernone und Valle Maggia. Schweiz. Mineral. Petrog. Mitt. **36**, 244–348 (1956)

Koeppel, V., Gruenenfelder, M.: A study of inherited and newly formed zircons from paragneisses and granitised sediments of the Strona-Ceneri zone (Southern Alps). Schweiz. Mineral. Petrog. Mitt. **51**, 387–411 (1971)

Koeppel, V.: Isotopic U-Pb ages of monazites and zircons from the crust-mantle transition and adjacent units of the Ivrea and Ceneri zones (Southern Alps, Italy). Contr. Mineral. and Petrol. (in press)

Koeppel, V., Sommerauer, J.: Trace elements and the behaviour of the U-Pb system in inherited and newly formed zircons. Contr. Mineral. and Petrol. (in press)
Krogh, T. E., Davis, G. L.: The Grenville front interpreted as an ancient plate boundary. Annual Report of the Director, Geophysical Laboratory, 239–240 (1971)
Kulp, J. L., Eckelmann, W. R.: Discordant U-Pb ages and mineral type. Am. Mineralogist **42**, 154–164 (1957)
McDowell, F. M.: Potassium-argon ages from the Ceneri zone, Southern Swiss Alps. Contr. Mineral. and Petrol. **28**, 165–182 (1970)
Milnes, A. G.: Structure and history of the Antigorio nappe (Simplon group, North Italy). Schweiz. Mineral. Petrog. Mitt. **45**, 167–177 (1965)
Naylor, R. S., Steiger, R. H., Wasserburg, G. J.: U-Th-Pb and Rb-Sr systematics in 2700 $\times$ 10^6 year old plutons from the Southern Wind River Range (Wyoming). Geochim. Cosmochim. Acta **34**, 1133–1159 (1970)
Niggli, E.: Alpine Metamorphose und alpine Gebirgsbildung. Fortschr. Mineral. **47**, 16–26 (1970)
Niggli, P., Preiswerk, H., Gruetter, O., Bosshard, L., Kuendig, R.: Geologische Beschreibung der Tessiner Alpen zwischen Maggia- und Bleniotal. Beitr. Geol. Karte Schweiz NF 71 (1936)
Pidgeon, R. T., Koeppel, V., Gruenenfelder, M.: U-Pb isotopic relationships in zircon suites from a para- and orthogneiss from the Ceneri zone, southern Switzerland. Contr. Mineral. and Petrol. **26**, 1–11 (1970)
Pidgeon, R. T., O'Neil, J. R., Silver, L. T.: Uranium and lead isotopic stability in a metamict zircon under experimental hydrothermal conditions. Science **154**, 1538–1540 (1966)
Silver, L. T.: The use of cogenetic uranium-lead isotope systems in zircons in geochronology. In: Radioactive Dating, Int. Atomic Energy Agency, Symp. Athens 1962, Proc., 279–287 (1963)
Silver, L. T., Deutsch, S.: Uranium-lead isotopic variations in zircons: a case study. J. Geol. **71**, 721–758 (1963)
Steiger, R. H., Baer, M. T., Buesch, W.: The zircon age of an anatectic rock in the central Black Forest. Fortschr. Mineral. **50**, Beiheft 3 (1972)
Steiger, R. H., Wasserburg, G. J.: Systematics in the ^{208}Pb-^{232}Th, ^{207}Pb-^{235}U and ^{206}Pb-^{238}U systems. J. Geophys. Res. **71**, 6065–6090 (1966)
Steiger, R. H., Wasserburg, G. J.: Comparative U-Th-Pb systematics in 2.7 $\times$ 10^9 year plutons of different geologic histories. Geochim. Cosmochim. Acta **33**, 1213–1232 (1969)
Stern, T. W., Goldich, S. S., Newell, M. F.: Effects of weathering on the U-Pb ages of zircon from the Morton gneiss, Minnesota. Earth Planet. Sci. Lett. **1**, 369–371 (1966)
Stern, T. W., Phair, G., Newell, M. F.: Boulder Creek batholith, Colorado. Part II: Isotopic age of emplacement and morphology of zircon. Bull. Geol. Soc. Am. **82**, 1615–1634 (1971)
Streckeisen, A.: In: Geologischer Führer der Schweiz, S. 337–346. Basel 1967
Tilton, G. R.: Volume diffusion as a mechanism for discordant lead ages. J. Geophys. Res. **65**, 2933–2945 (1960)
Tilton, G. R., Wetherill, G. W., Davis, G. L., Hopson, C. A.: Ages of minerals from the Baltimore gneiss near Baltimore, Maryland. Bull. Geol. Soc. Am. **69**, 1469–1474 (1958)
Ulrych, T. J.: Discordant lead-uranium ages due to continuous loss of lead. Nature **200**, 561–562 (1963)
Vitrac, A., Allègre, C. J.: Datation ^{87}Rb-^{87}Sr des gneiss du Canigou et de l'Agly (Pyrénées Orientales, France), Compt. Ren. **273**, 2411–2413 (1971)
Wasserburg, G. J.: Diffusion processes in lead-uranium systems. J. Geophys. Res. **68**, 4823–4846 (1963)
Wenk, E.: Ergebnisse und Probleme der Gefügeuntersuchungen im Verzascatal (Tessin). Schweiz. Mineral. Petrog. Mitt. **23**, 265–294 (1943)
Wenk, E.: In: Geologischer Führer der Schweiz, S. 348–350. Basel 1967
Wenk, E.: Zur Regionalmetamorphose und Ultrametamorphose im Lepontin. Fortschr. Mineral. **47**, 34–51 (1970)
Wetherill, G. W.: Discordant uranium-lead ages. Trans. Geophys. Union **37**, 320–326 (1956)
Wetherill, G. W.: Discordant uranium-lead ages, part 2: discordant ages resulting from diffusion of lead and uranium. J. Geophys. Res. **68**, 2957–2965 (1963)

Dr. V. Köppel
Institut für Kristallographie
Sonneggstr. 5, CH-8006 Zürich, Switzerland